PHILOSOPHICAL TRANSACTIONS OF THE ROYAL SOCIETY A MATHEMATICAL, PHYSICAL & ENGINEERING SCIENCES

Observable effects of Ca^{2+} buffers on local Ca^{2+} signals

Guillermo Solovey and Silvina Ponce Dawson

Phil. Trans. R. Soc. A 2010 **368**, 5597-5603
doi: 10.1098/rsta.2010.0273

PHILOSOPHICAL TRANSACTIONS OF THE ROYAL SOCIETY A

Phil. Trans. R. Soc. A (2010) **368**, 5597–5603
doi:10.1098/rsta.2010.0273

Observable effects of Ca^{2+} buffers on local Ca^{2+} signals

By Guillermo Solovey[1,2] and Silvina Ponce Dawson[2,*]

[1]*Laboratory of Mathematical Physics, Rockefeller University, 1230 York Avenue, New York, NY 10065, USA*
[2]*Departamento de Física, Facultad de Ciencias Exactas y Naturales, Universidad de Buenos Aires, Pabellón I, Ciudad Universitaria, 1428 Buenos Aires, Argentina*

Calcium signals participate in a large variety of physiological processes. In many instances, they involve calcium entry through inositol 1,4,5-trisphosphate (IP_3) receptors (IP_3Rs), which are usually organized in clusters. Recent high-resolution optical experiments by Smith & Parker have provided new information on Ca^{2+} release from clustered IP_3Rs. In the present paper, we use the model recently introduced by Solovey & Ponce Dawson to determine how the distribution of the number of IP_3Rs that become open during a localized release event may change by the presence of Ca^{2+} buffers, substances that react with Ca^{2+}, altering its concentration and transport properties. We then discuss how buffer properties could be extracted from the observation of local signals.

Keywords: Ca^{2+}; puffs; buffers

1. Introduction

Calcium signals participate in a large variety of physiological processes (Berridge *et al.* 1998). At basal conditions, free cytosolic [Ca^{2+}] is very low (approx. 100 nM). It is much higher in the extracellular medium and in internal reservoirs, such as the endoplasmic reticulum (ER). Ca^{2+} entry in the cytosol through specific channels that become open upon stimulation is the basic component of Ca^{2+} signals. This change in cytosolic [Ca^{2+}] is then translated into different end responses depending on the cell type and on the resulting spatio-temporal distribution of [Ca^{2+}]. Thus, it is of interest to determine how different factors affect this distribution.

One of the Ca^{2+} channels involved in intracellular Ca^{2+} signals is the inositol 1,4,5-trisphosphate (IP_3) receptor (IP_3R). It is located on the surface of intracellular membranes, particularly, of the ER. IP_3Rs are biphasically regulated by Ca^{2+}. For this reason, kinetic models of the receptor assume that there is at least one activating and one inhibitory Ca^{2+}-binding site, so that Ca^{2+} binding to the first one induces channel opening (provided that IP_3 is also bound to the IP_3R)

*Author for correspondence (silvina@df.uba.ar).

One contribution of 13 to a Theme Issue 'Complex dynamics of life at different scales: from genomic to global environmental issues'.

while binding to the second one induces channel closing (De Young & Keizer 1992; Fraiman & Ponce Dawson 2004; Shuai *et al.* 2007). The affinity for Ca^{2+} of the activating site is larger than that of the inhibitory site. In this way, Ca^{2+}-induced Ca^{2+} release (CICR) occurs in which the Ca^{2+} ions released through an open channel induce the opening of other nearby channels with IP_3 bound.

IP_3Rs are not uniformly distributed on the membrane of the ER. They are organized in clusters separated by a few micrometres (Yao *et al.* 1995; Smith & Parker 2009). The combination of this inhomogeneity and of CICR gives rise to a large variety of intracellular Ca^{2+} signals, which go from local ones such as 'blips' (Ca^{2+} release through a single IP_3R) and 'puffs' (Ca^{2+} release through several IP_3Rs in a cluster) to waves that propagate throughout the cell (Sun *et al.* 1998). These signals have been observed using fluorescence microscopy and Ca^{2+}-sensitive dyes (Bootman *et al.* 1997; Callamaras *et al.* 1998; Sun *et al.* 1998), and various models have been presented to interpret the observations (Swillens *et al.* 1999; Shuai *et al.* 2006; Swaminathan *et al.* 2009; Thul *et al.* 2009; Bruno *et al.* 2010). The use of total internal reflection fluorescence (TIRF) microscopy and a fast charge-coupled device camera in intact mammalian cells represents an experimental breakthrough that is giving more direct information on intracluster properties (Smith & Parker 2009). In particular, the distribution of the number of channels that open during puffs can be obtained without much processing. By keeping data that come from clusters of similar size, it is possible to get rid of cluster-to-cluster variability and obtain a distribution that provides an insight into the intracluster Ca^{2+} dynamics during puffs. We have recently presented a simple model with which we could reproduce the distribution reported in Smith & Parker (2009) and interpret its shape in terms of the competition of two stochastic processes: IP_3 binding and Ca^{2+}-mediated interchannel coupling (Solovey & Ponce Dawson 2010).

Interchannel coupling is mediated by the Ca^{2+} released through an open IP_3R that subsequently diffuses to a neighbouring channel. This interaction may be affected by the presence of Ca^{2+} buffers that change the effective mobility and concentration of free Ca^{2+} ions (Allbritton *et al.* 1992). Cells contain a wide variety of these substances, particularly, Ca^{2+}-binding proteins, which are often selectively expressed in specific subpopulations or at certain stages during the cell life. Exogenous buffers, on the other hand, can be used as an experimental tool to perturb Ca^{2+} signals at time and distance scales inaccessible to direct visualization (Dargan & Parker 2003). In this paper, we use the model introduced in Solovey & Ponce Dawson (2010) to analyse how the addition of exogenous buffers may affect the distribution of the number of channels that open during puffs. This study shows how the applicability and limitations of the model of Solovey & Ponce Dawson (2010) may be tested experimentally. It also shows how information on the effect of Ca^{2+} buffers on the intracluster dynamics may be extracted in experiments from the observed puff-size distribution.

The organization of the paper is as follows. In §2, we explain the main features of the model introduced in Solovey & Ponce Dawson (2010). In §3, we study numerically how the addition of different amounts of exogenous buffers affects the communication between channels, and we determine how the parameters of the model of Solovey & Ponce Dawson (2010) should be varied accordingly.

Based on this, in §4, we study how the puff-size distribution given by the model of Solovey & Ponce Dawson (2010) changes with the addition of buffers. The conclusions are summarized in §5.

2. The model

In this section, we summarize the main features of the model introduced in Solovey & Ponce Dawson (2010) to describe the distribution of puff sizes reported in Smith & Parker (2009). Based on previous analyses (Bruno *et al.* 2010), the model assumes that a cluster occupies a circle of fixed radius, $R = 250\,\mathrm{nm}$, and that N IP_3Rs are randomly distributed inside it with uniform probability. The model has been developed for data collected from similar-type clusters, so that the value of N is also fixed. In the model, each IP_3R of a cluster has a probability p of having IP_3 bound, and if an IP_3R becomes open it induces the opening of all other *available* IP_3Rs (i.e. with IP_3 bound) within a distance r_{inf} of it, giving rise to a puff. These newly opened IP_3Rs in turn trigger the opening of new IP_3Rs with IP_3 bound that are within the distance r_{inf} from an open one. This scheme gives rise to a cascade of openings that stops when there are no more available IP_3Rs within the radius of influence (i.e. the distance r_{inf}) of any open IP_3R. This implies that each puff is characterized by two random variables: the number of available IP_3Rs, N_p, and the number of open IP_3Rs, n. The values that N_p can take on depend on N and p. The latter is proportional to $[IP_3]$. The values that n can take on depend on N_p and on the spatial extent of CICR represented by r_{inf}. The probability that an available IP_3R makes a transition to the open state is an increasing function of the $[Ca^{2+}]$ it senses. The $[Ca^{2+}]$ profile around an open IP_3R, on the other hand, is a decreasing function of the distance to the Ca^{2+} source that depends on the Ca^{2+} current and on the factors that interfere with Ca^{2+} transport (e.g. buffers). Having a fixed value of r_{inf} carries the assumption that the Ca^{2+} profile around an open IP_3R is the same regardless of how many of them are simultaneously open in the cluster (see Solovey *et al.* (2008) for a discussion on this).

Given a cluster, the model generates a sequence of puffs by determining, for each of them, which of the N IP_3Rs are available, which one is the first to become open and then applying the rule that all available IP_3Rs within a distance r_{inf} of an open one become open. The probability, P_n, of having a puff with n open channels can then be written as

$$P_n = \sum_{N_p \geq n}^{N} P_{\mathrm{o}}\left(\frac{n}{N_p}\right) P_{\mathrm{A}}(N_p), \quad n \geq 1, \tag{2.1}$$

where $P_{\mathrm{A}}(N_p)$ is the probability that there are N_p available IP_3Rs before the occurrence of the puff and $P_{\mathrm{o}}(n/N_p)$ is the conditional probability that n channels open given that there are N_p available IP_3Rs. Equation (2.1) highlights the two stochastic components that shape P_n: IP_3 binding (described by $P_{\mathrm{A}}(N_p)$) and Ca^{2+}-mediated interchannel coupling (described by $P_{\mathrm{o}}(n/N_p)$). The relative weight of both factors depends on the relationship between two typical length scales of the problem: the radius of influence, r_{inf}, and the mean distance between available IP_3Rs, D, which is a random variable that is given by $D = R/2\sqrt{(\pi/N_p)}$.

If, for most events, the values of N_p are such that r_{inf}/D is very large, then the opening of any IP_3R of the cluster leads to the opening of all available IP_3Rs. In such a case, $P_o(n/N_p) \approx \delta_{nN_p}$ and $P_n \approx P_A(n)$, which is a binomial. On the other hand, if r_{inf}/D is small for most events, then P_n is concentrated near $n = 1$, regardless of how many available IP_3Rs there are in each realization. We refer to these two extreme cases as IP_3 and Ca^{2+} limited, respectively. In between these extreme cases, one or the other behaviour may be favoured depending on the value of N_p, i.e. on the realization. In such a case, the dominant stochastic component of P_n depends on the value of n.

3. Intracluster Ca^{2+} distribution in the presence of different buffers

In this section, we study how the addition of exogenous Ca^{2+} buffers affects the Ca^{2+}-mediated channel–channel interaction. The aim is to determine how r_{inf} should be varied in the model to account for the presence of these added buffers. To this end, we simulate the reaction–diffusion system that models the dynamics of cytosolic Ca^{2+} as described in Solovey *et al.* (2008) in the presence of one open IP_3R. An open IP_3R is considered to be a point source that releases a constant Ca^{2+} current that was estimated from experimental data to be 0.1 pA (Bruno *et al.* 2010). The reaction–diffusion system (Solovey *et al.* 2008) also includes a cytosolic Ca^{2+} indicator dye and an exogenous buffer, either ethylene glycol tetraacetic acid (EGTA) or bis(2-aminophenoxy)ethane tetraacetic acid (BAPTA). The Ca^{2+} indicator represents the dye usually used in fluorescent microscopy experiments and exogenous buffers are used in experiments to prevent the initiation of Ca^{2+} waves. We repeat the simulations for different amounts of the exogenous buffer and compare the $[Ca^{2+}]$ distributions obtained. The simulated equations are

$$\left.\begin{aligned} \frac{\partial [Ca^{2+}]}{\partial t} &= D_{Ca}\nabla^2[Ca^{2+}] - \sum_X R_{CaX} + \sigma\delta(r), \\ \frac{\partial [F]}{\partial t} &= D_F\nabla^2[F] - R_{CaF}, \\ \frac{\partial [B]}{\partial t} &= D_B\nabla^2[B] - R_{CaB} \\ \text{and} \qquad \frac{\partial [E]}{\partial t} &= -R_{CaE}, \end{aligned}\right\} \tag{3.1}$$

where F is the Ca^{2+} dye used in the experiments, B is the exogenous buffer (B = EGTA or BAPTA), σ is proportional to the Ca^{2+} current and E is an immobile species that accounts for the effect of all endogenous buffers. In equations (3.1), the reaction terms are of the form $R_{CaX} = k_{on}^X[Ca^{2+}][X] - k_{off}^X([X]_T - [X])$ with $X = E, F, B$ and $[X]_T$ is the total concentration of the corresponding species. The parameter values are as in Solovey *et al.* (2008): $D_{Ca} = 220\,\mu m^2\,s^{-1}$, $D_F = 15\,\mu m^2\,s^{-1}$, $k_{on}^E = 400\,\mu M^{-1}\,s^{-1}$, $k_{off}^E = 500\,s^{-1}$, $[E]_T = 300\,\mu M$, $k_{on}^F = 150\,\mu M^{-1}\,s^{-1}$, $k_{off}^F = 300\,s^{-1}$ and $[F]_T = 25\,\mu M$. For B = EGTA we consider $k_{on}^B = 5\,\mu M^{-1}\,s^{-1}$ and $k_{off}^B = 0.75\,s^{-1}$ and for B = BAPTA, $k_{on}^B = 600\,\mu M^{-1}\,s^{-1}$ and $k_{off}^B = 100\,s^{-1}$.

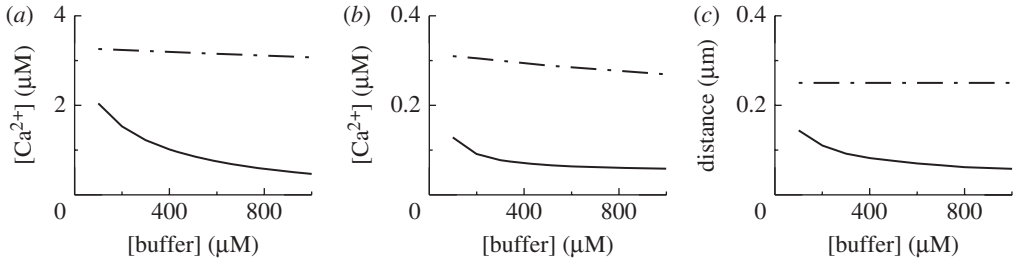

Figure 1. (*a*) Cytosolic $[Ca^{2+}]$ at a distance $r = 0.05\,\mu m$ from a 0.1 pA point source in the presence of EGTA (dot-dashed line) or BAPTA (solid line) as a function of the corresponding exogenous total buffer concentration. (*b*) Similar to (*a*) but at $r = 0.25\,\mu m$. (*c*) Distance r at which $[Ca^{2+}] = 0.3\,\mu M$ in the presence of different amounts of $[BAPTA]_T$ (solid line). The dot-dashed line is set at $r = 0.25\,\mu m$, the distance at which $[Ca^{2+}] \approx 0.3\,\mu M$ in the presence of the amounts of EGTA considered here.

We perform the simulations using a forward Euler method in time and finite differences in space with a second-order expression for the Laplacian. We use spherical coordinates, and the simulation domain is a 2 μm radius sphere. The boundary conditions are no-flux at $r = 2\,\mu m$. We perform simulations for $[B]_T$ between 100 μM and 1 mM for both EGTA and BAPTA.

Clusters have been estimated to be $400 \times 400\,nm$ in size (Shuai *et al.* 2006; Smith & Parker 2009; Bruno *et al.* 2010) while typical interchannel distances are assumed to be around 20 nm (Ur-Rahman *et al.* 2009). The model described in §2 reproduces the observations of Smith & Parker (2009) for $r_{inf} = 0.25\,\mu m$. Thus, for exogenous buffers to alter interchannel communication they need to be fast enough (Zeller *et al.* 2009) so that they act over time scales shorter than 0.3 ms (the typical time it takes for Ca^{2+} to diffuse over a 0.25 μm distance). EGTA is a slow buffer while BAPTA is fast. Their different effects on the intracluster Ca^{2+} dynamics are evident in figure 1 where we have plotted $[Ca^{2+}]$ at a distance $r = 0.05\,\mu m$ (figure 1*a*) and $r = 0.25\,\mu m$ (figure 1*b*) from the open IP_3R in the presence of EGTA (dot-dashed line) or BAPTA (solid line) as functions of the corresponding exogenous total buffer concentration. We observe that $[Ca^{2+}]$ at both distances is very insensitive to the addition of EGTA ($[Ca^{2+}](0.05\,\mu m) \approx 3.1\,\mu M$ and $[Ca^{2+}](0.25\,\mu m) \approx 0.3\,\mu M$ for all $[EGTA]_T$) while it is significantly altered by the presence of BAPTA. Considering that the probability per unit time that an available IP_3R makes a transition to the open state is proportional to $[Ca^{2+}]$, then the ratio of $[Ca^{2+}]$ at a given distance in the presence of BAPTA and in the presence of EGTA gives an estimate of the factor by which r_{inf} should be multiplied in the presence of one or the other buffer. This ratio ranges between 0.66 and 0.15 at $r = 0.05\,\mu m$ and between 0.45 and 0.2 at $r = 0.25\,\mu m$. Taking into account that $r_{inf} = 0.25\,\mu m$ is the value at which the model of Solovey & Ponce Dawson (2010) reproduces the observations of Smith & Parker (2009), which were obtained in the presence of moderate amounts of EGTA and given that $[Ca^{2+}](0.25\,\mu m) \approx 0.3\,\mu M$ for all the values of $[EGTA]_T$ considered here, we can also estimate r_{inf} in the presence of BAPTA as the distance from the 0.1 pA source at which $[Ca^{2+}] = 0.3\,\mu M$ for the simulations with BAPTA. We show this distance as a function of $[BAPTA]_T$ in figure 1*c*. The ratio of this distance to 0.25 μm varies between 0.58 and 0.23 for the values of $[BAPTA]_T$ considered.

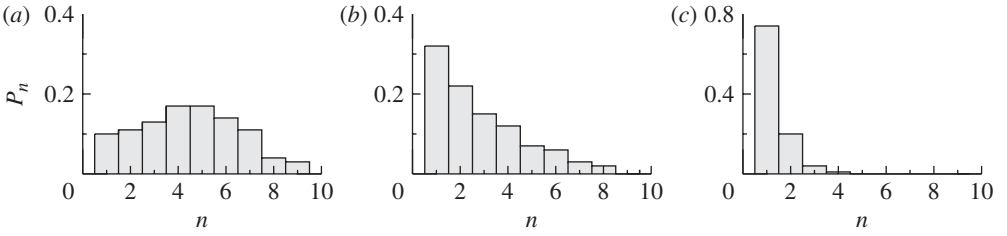

Figure 2. Probability, P_n, of having a puff with n open channels obtained with 1000 realizations of our model for $N = 18$, $p = 5/18$, $R = 250\,\mathrm{nm}$ and different values of r_{inf}: (*a*) $r_{\mathrm{inf}} = 250\,\mathrm{nm}$, the value that reproduces the observations of Smith & Parker (2009) obtained in the presence of EGTA only; (*b*) $r_{\mathrm{inf}} = 160\,\mathrm{nm}$, the value of this parameter in the presence of $[\mathrm{BAPTA}]_{\mathrm{T}} = 100\,\mu\mathrm{M}$; and (*c*) $r_{\mathrm{inf}} = 70\,\mathrm{nm}$, the value of this parameter in the presence of $[\mathrm{BAPTA}]_{\mathrm{T}} = 500\,\mu\mathrm{M}$.

4. The effect of Ca^{2+} buffers on P_n

The studies of the previous section illustrated in figure 1 consistently indicate that the value $r_{\mathrm{inf}} = 0.25\,\mu\mathrm{m}$ estimated in Solovey & Ponce Dawson (2010) should be decreased by a factor between 0.6 and 0.2 to account for the presence of BAPTA with total concentrations between 100 µM and 1 mM. We show in figure 2 the distribution, P_n, obtained with the model for $r_{\mathrm{inf}} = 0.25\,\mu\mathrm{m}$ (figure 2*a*), $r_{\mathrm{inf}} = 0.16\,\mu\mathrm{m}$ (figure 2*b*) and $r_{\mathrm{inf}} = 0.07\,\mu\mathrm{m}$ (figure 2*c*), which correspond to situations with EGTA, $[\mathrm{BAPTA}]_{\mathrm{T}} = 100\,\mu\mathrm{M}$ and $[\mathrm{BAPTA}]_{\mathrm{T}} = 500\,\mu\mathrm{M}$, respectively. We observe in this figure that the addition of 100 µM BAPTA already introduces a noticeable change in the observed distribution of puff sizes, P_n. The distribution for $[\mathrm{BAPTA}]_{\mathrm{T}} = 500\,\mu\mathrm{M}$ is highly concentrated around $n = 1$ (with $P_n = 0$ for $n \leq 4$), a situation that is even more pronounced for $[\mathrm{BAPTA}]_{\mathrm{T}} = 1\,\mathrm{mM}$ (data not shown).

5. Conclusions

We have combined the results of numerical simulations of intracellular Ca^{2+} dynamics with the model introduced in Solovey & Ponce Dawson (2010) to determine how the distribution of the number of IP_3Rs that become open during Ca^{2+} puffs may change by the presence of different Ca^{2+} buffers. In particular, we have determined that the addition of 100 µM of a fast buffer such as BAPTA may introduce noticeable effects on the observed distribution. Adding such a fast buffer could decrease the amplitude of the smallest puffs below the threshold of detection. However, this is not likely to happen for 100 µM. Thus, we suggest to perform experiments as in Smith & Parker (2009) but in the presence of different amounts of BAPTA (up to 100 µM) to probe the model of Solovey & Ponce Dawson (2010) and to extract information on how the spatial extent of CICR varies with this buffer.

This research was supported by UBA (UBACyT X145), ANPCyT (PICT 17-21001), Santa Fe Institute and CONICET (PIP 112-200801-01612).

References

Allbritton, N. L., Meyer, T. & Stryer, L. 1992 Range of messenger action of calcium ion and inositol 1,4,5-triphosphate. *Science* **258**, 1812–1815. (doi:10.1126/science.1465619)

Berridge, M. J., Bootman, M. D. & Lipp, P. 1998 Calcium—a life and death signal. *Nature* **395**, 645–648. (doi:10.1038/27094)

Bootman, M. D., Berridge, M. J. & Lipp, P. 1997 Cooking with calcium: the recipes for composing global signals from elementary events. *Cell* **91**, 367–373. (doi:10.1016/S0092-8674(00)80420-1)

Bruno, L., Solovey, G., Ventura, A. C., Dargan, S. & Ponce Dawson, S. 2010 Quantifying calcium fluxes underlying calcium puffs in *Xenopus laevis* oocytes. *Cell Calcium* **47**, 273–286. (doi:10.1016/j.ceca.2009.12.012)

Callamaras, N., Marchant, J. S., Sun, X.-P. & Parker, I. 1998 Activation and co-ordination of InsP_3-mediated elementary Ca^{2+} events during global Ca^{2+} signals in *Xenopus* oocytes. *J. Physiol.* **509**, 81–91. (doi:10.1111/j.1469-7793.1998.081bo.x)

Dargan, S. L. & Parker, I. 2003 Buffer kinetics shape the spatiotemporal patterns of IP_3-evoked Ca^{2+} signals. *J. Physiol.* **553**, 775–788. (doi:10.1113/jphysiol.2003.054247)

De Young, G. W. & Keizer, J. 1992 A single-pool inositol 1,4,5-triphosphate-receptor-based model for agonist-stimulated oscillations in Ca^{2+} concentration. *Proc. Natl Acad. Sci. USA* **89**, 9895–9899. (doi:10.1073/pnas.89.20.9895)

Fraiman, D. & Ponce Dawson, S. 2004 A model of the IP_3 receptor with a luminal calcium binding site: stochastic simulations and analysis. *Cell Calcium* **35**, 403–413. (doi:10.1016/j.ceca.2003.10.004)

Shuai, J., Rose, H. J. & Parker, I. 2006 The number and spatial distribution of IP_3 receptors underlying calcium puffs in *Xenopus* oocytes. *Biophys. J.* **91**, 4033–4044. (doi:10.1529/biophysj.106.088880)

Shuai, J., Pearson, J. E., Foskett, J. K., Mak, D.-O. D. & Parker, I. 2007 A kinetic model of clustered IP_3 receptors in the absence of Ca^{2+} feedback. *Biophys. J.* **93**, 1151–1162. (doi:10.1529/biophysj.107.108795)

Smith, I. F. & Parker, I. 2009 Imaging the quantal substructure of single IP_3R channel activity during Ca^{2+} puffs in intact mammalian cells. *Proc. Natl Acad. Sci. USA* **106**, 6404–6409. (doi:10.1073/pnas.0810799106)

Solovey, G. & Ponce Dawson, S. 2010 Intra-cluster percolation of calcium signals. *PLoS ONE* **5**, e8997. (doi:10.1371/journal.pone.0008997)

Solovey, G., Fraiman, D., Pando, B. & Ponce Dawson, S. 2008 Simplified model of cytosolic Ca^{2+} dynamics in the presence of one or several clusters of Ca^{2+}-release channels. *Phys. Rev. E* **78**, 041915. (doi:10.1103/PhysRevE.78.041915)

Sun, X.-P., Callamaras, N., Marchant, J. S. & Parker, I. 1998 A continuum of InsP_3-mediated elementary Ca^{2+} signalling events in *Xenopus* oocytes. *J. Physiol.* **509**, 67–80. (doi:10.1111/j.1469-7793.1998.067bo.x)

Swaminathan, D., Ullah, G. & Jung, P. 2009 A simple sequential-binding model for calcium puffs. *Chaos* **19**, 037109. (doi:10.1063/1.3152227)

Swillens, S., Dupont, G., Combettes, L. & Champeil, P. 1999 From calcium blips to calcium puffs: theoretical analysis of the requirements for interchannel communication. *Proc. Natl Acad. Sci. USA* **96**, 13 750–13 755. (doi:10.1073/pnas.96.24.13750)

Thul, R., Thurley, K. & Falcke, M. 2009 Toward a predictive model of Ca^{2+} puffs. *Chaos* **19**, 037108. (doi:10.1063/1.3183809)

Ur-Rahman, T., Skupin, A., Falcke, M. & Taylor, C. W. 2009 Clustering of $InsP_3$ receptors by $InsP_3$ retunes their regulation by $InsP_3$ and Ca^{2+}. *Nature* **458**, 655–659. (doi:10.1038/nature07763)

Yao, Y., Choi, J. & Parker, I. 1995 Quantal puffs of intracellular Ca^{2+} evoked by inositol trisphosphate in *Xenopus* oocytes. *J. Physiol.* **482**, 533–553.

Zeller, S., Rüdiger, S., Engel, H., Sneyd, J., Warnecke, G., Parker, I. & Falcke, M. 2009 Modeling of the modulation by buffers of Ca^{2+} release through clusters of IP_3 receptors. *Biophys. J.* **97**, 992–1002. (doi:10.1016/j.bpj.2009.05.050)